Edge-Illumination X-ray Phase Contrast Imaging with Pt-based Metallic Glass Masks

Somayeh Saghamanesh [1*], Seyed Mahmoodreza Aghamiri [1], Alessandro Olivo [2], Maryam Sadeghilarijani [3], Hidemi Kato [4], Alireza Kamali-asl [1], and Wataru Yashiro [3]

[1] Department of Medical Radiation Engineering, Shahid Beheshti University, Tehran, 1983969411, Iran.

[2] Department of Medical Physics and Bioengineering, University College London, Malet Place, Gower Street, London WC1E 6BT, UK

[3] Institute of Multidisciplinary Research for Advanced Materials (IMRAM), Tohoku University, Sendai 980-8577, Japan

[4] Institute for Materials Research (IMR), Tohoku University, Sendai 980-8577, Japan

* Corresponding author: E-mail: s_saghamanesh@sbu.ac.ir

Abstract

Edge-Illumination X-ray phase contrast imaging (EI XPCI) is a non-interferometric phase-sensitive method where two absorption masks are employed. These masks are fabricated through a photolithography process followed by electroplating which is challenging in terms of yield as well as time- and cost-effectiveness. We report on the first implementation of EI XPCI with Pt-based metallic glass masks fabricated by an imprinting method. The new tested alloy exhibits good characteristics including high workability beside high X-ray attenuation. The fabrication process is easy and cheap, and can produce large-size masks for high X-ray energies within minutes. Imaging experiments show a good quality phase image, which confirms the potential of these masks to make the EI XPCI technique widely available and affordable.

An alternative approach to X-ray attenuation imaging, called X-ray phase contrast imaging (XPCI), has generated a new trend in the area of X-ray imaging and microscopy in last two decades[1–3]. This technique provides complementary information about structures that create measurable phase shifts of X-rays upon interaction but don't necessarily exhibit detectable absorption differences. It has demonstrated superior contrast and visibility compared to conventional absorption X-ray imaging and has shown potential in many applications from biomedicine to material science[4]. Among different XPCI methods,[5–12] we

focus on the edge illumination (EI) technique,[13] which could extend the capability of extracting phase information to common laboratory X-ray sources[14]. This extension, sometimes referred to as coded-aperture (CA) XPCI, has a non-interferometric nature with a simple setup[15]. In this method two sets of absorption gratings, usually called masks, are used to implement the edge illumination condition with incoherent and polychromatic X-ray sources over large field of views (FOVs) (see Figure 1). These masks can be created as one-dimensional[16] or two-dimensional patterns[17] to produce phase sensitivity in one or two directions, respectively; asymmetric mask designs can also be realized to obtain multi-modal (attenuation, phase, dark-field) images through a single scan for the sample, or by sacrificing some degree of spatial resolution in non-scanning systems[18].

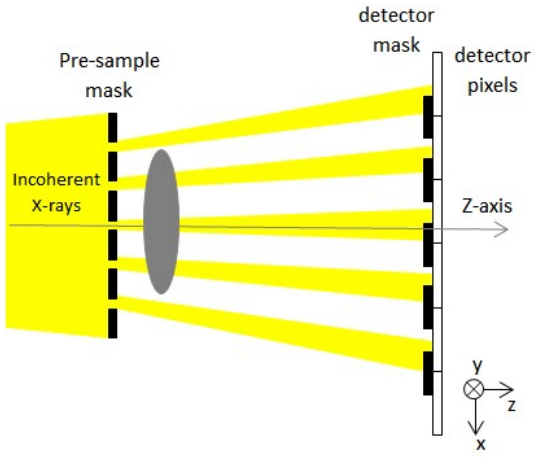

FIG. 1. A schematic setup of an extended edge-illumination X-ray phase contrast imaging system (i.e. coded-aperture XPCI).

As can be seen in Figure 1, the pre-sample mask acts as an array of apertures and creates small beamlets incident on the detector mask, which blocks part of the radiation impinging on the detector pixels. The magnified pitch of the pre-sample mask is matched to the pitch of the detector mask. The relative displacement of two masks along the x-axis results in an illumination fraction which determines the phase sensitivity of this XPCI system, and allows phase signal extraction from only two complementary positions of those masks[19].

The common fabrication procedure for these masks consists of a photolithography process followed by electroplating where heavy elements such as gold are usually used[20]. A number of techniques have been proposed to fabricate X-ray absorption gratings/masks as well as increase their performance, most of which were through the LIGA process[21–24]. They

have mainly attempted to increase the height to pitch ratio (aspect ratio) or field of view of gratings but realizing both goals at the same time has posed severe difficulties[25–29]. In fact, the smaller the pitch of these gratings, the more the fabrication process becomes difficult in electroforming, since achieving a uniform and relatively defect-free pattern requires considerable time and cost. Especially high X-ray energies demand higher aspect ratios and therefore, producing high yield gratings in desired large size is still challenging, even for large pitches.

However, a few other approaches have been suggested for grating fabrication. In a study, a hard X-ray multiple slice was proposed through a stacked-sliced technique for grating interferometry, where Al and Ta foils were used[30]. Also a multilayer deposition approach has been reported to achieve X-ray gratings with a sub-micron pitch but low aspect ratio and small area[31]. In a work, an imprinting method was proposed to fabricate low cost Pd-based metallic glass absorption gratings in a fast manner[32]. Another research work used Gd element to produce absorption grating for the X-ray and neutron grating interferometry[33]. Some researchers adopted a micro-casting approach to produce X-ray absorption gratings with Bismuth at low cost[34,35].

In this paper, we present the first EI XPCI system built with metallic-glass masks fabricated by an imprinting machine. Also for the first time, Pt has been used as an excellent x-ray absorber in the fabrication of X-ray gratings for phase imaging purposes. The masks were produced within a few minutes. The process can be used to fabricate thick masks suitable for imaging large samples at high x-ray energy and low cost as well.

II. FABRICATION TECHNIQUE

The fabrication process was based on imprinting, which is a well-established method for manufacturing compact disks (CDs), digital versatile disks (DVDs), diffraction gratings, and polymer components[36]. Nanoimprinting represents the fabrication of micro- and nano-devices by embossing features from a hard mold onto thermoplastic materials such as metallic glasses in their super-cooled liquid region (SCLR) [37,38].

In this work, two absorption masks were designed according to an EI XPCI system described in the next section. The fabrication procedure was performed in two steps. In the first step, two Si wafers with a thickness of 200 μm and diameter of 10 cm were prepared and processed through the inductively-coupled plasma (ICP) etching. In this process, two masks were patterned with a depth of 43 μm and a 40 × 40-mm^2 area on which pitches of 72 μm and 106 μm were created for the pre-sample and detector mask, respectively.

In the next step, the metallic glass material was prepared. The alloy $Pt_{60}Ni_{15}P_{25}$ (density ≈12.51 $g.cm^{-3}$) was made by inductively melting pure elements of Pt, Ni, and P in quartz tubes. Then, the alloy was exposed to a fluxing treatment process. B_2O_3 was added to the alloy and heated up to about 900 K for 60 min. One reason to select this composition is its high content of Pt which can absorb X-rays effectively and is thus well suited to be used in X-ray absorption gratings; another reason is its high workability at the minimum viscosity of $\sim 10^{5\text{-}6}$ Pa s in the supercooled liquid temperature region. This property provides higher formability compared to other previous attempted alloys like Gd-based metallic glass (Gd-MG) [32]. In other words, Pt-MG requires less pressure and temperature than Gd-MG and thus can remain in the glassy state instead of turning into a crystal. However, Gd-MG would be crystallized in high temperatures and need higher pressures, which may lead to the breakage of the machine's plate or mold.

Glassy ribbons with a thickness of ~ 40-50 μm and width of ~ 10 mm were prepared in an argon atmosphere by the single roller melt spinning technique.

The imprinting process was performed using a nanoimprinting machine. The 10 × 45-mm^2 Pt-based metallic glass ribbons were placed on the mold and sandwiched by two ceramic heaters. Then, they were heated up to 300 °C and pressed into the mold under a load of 2 kN (~ 5 MPa) in an inactive gas ambient. Figure 2 represents the schematic of the mask fabrication process. Some additional finishing treatments such as surface polishing can be performed to enhance the masks' uniformity and x-ray transmission.

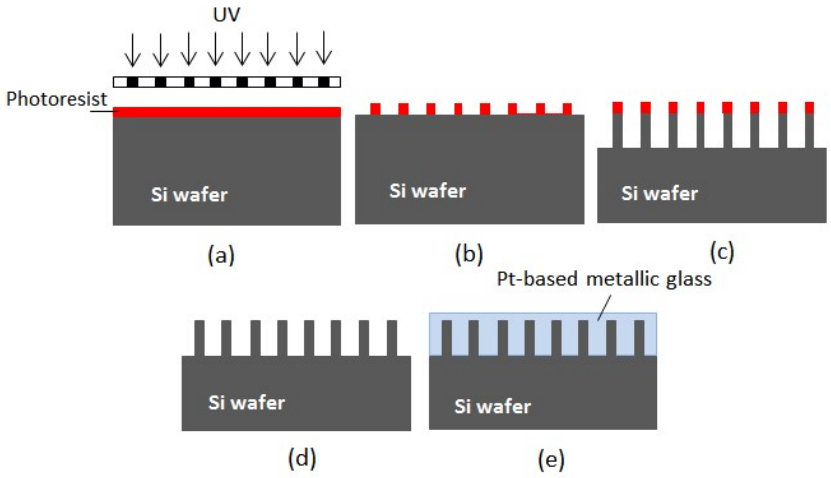

FIG. 2. A schematic fabrication process of CA masks: (a) substrate preparation using a positive photoresist and subsequent selective UV exposure, (b) pattern transfer on the wafer, (c) ICP etching, (d) photoresist removal and mold preparation, (e) imprinting the metallic glass into the mold.

III. EXPERIMENTAL TEST

To examine the performance of the fabricated masks, a coded-aperture imaging system was set up according to the design parameters, as depicted in Figure 1. A micro-focus X-ray source (Hamamatsu Photonics L9181S) was employed with a Tungsten target. The tube was operated at 30 kV_p and 300 μA. The largest available focal spot size of 40 μm was selected. A molybdenum sheet (0.050 mm) was used to give a mean spectral energy of approximately 17.5 keV. The output of the used X-ray energy spectrum has been simulated as shown in Figure 3.

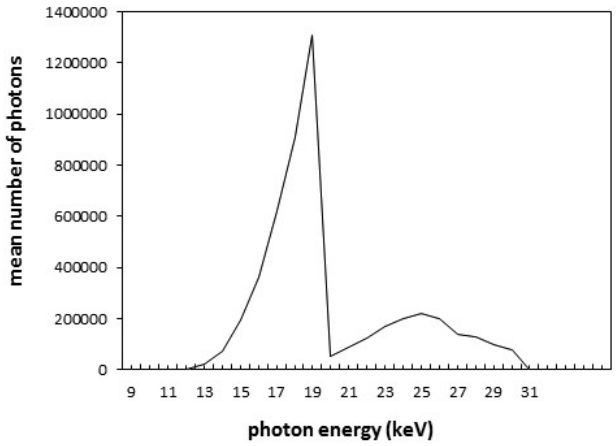

FIG. 3. The output of an X-ray source (in arbitrary unit) with a Tungsten target and Molybdenum filter at 30 kV_p.

The fabricated pre-sample mask and detector mask were placed at about 84 cm and 124 cm from the source, respectively. A scintillation detector (Spectral Instruments 1000 series) was placed closely behind the detector mask. The thickness of the scintillator (GADOX) was 40 μm, coupled to a CCD chip of 4096 x 4096 pixels by 1:2 fiber bundles. The effective pixel size was 18 μm.

After alignment of the masks, the pre-sample mask was translated relative to the detector mask along the x-axis by 4-μm increments to obtain the illumination curve of this system over an entire pitch. Four different rubber cylinders were selected as samples for testing these new masks at 30 kV_p. The sample was placed immediately downstream the pre-sample mask. Two image frames were acquired at opposite positions on the illumination curve (see Figure 5), each corresponding to 50% of illumination fraction. These two frames were used to retrieve the absorption and differential phase image through the curve inversion method [39].

IV. RESULTS AND DISCUSSION

Figure 4(a) displays the 3D image of a Si mold obtained by a laser confocal microscope. A scanning electron microscopy (SEM) image of the Pt- metallic glass mask fabricated by the imprinting method is shown in Figure 4(b). The full penetration of the metallic glass into the Si mold and successful realization of the masks were verified by the SEM image.

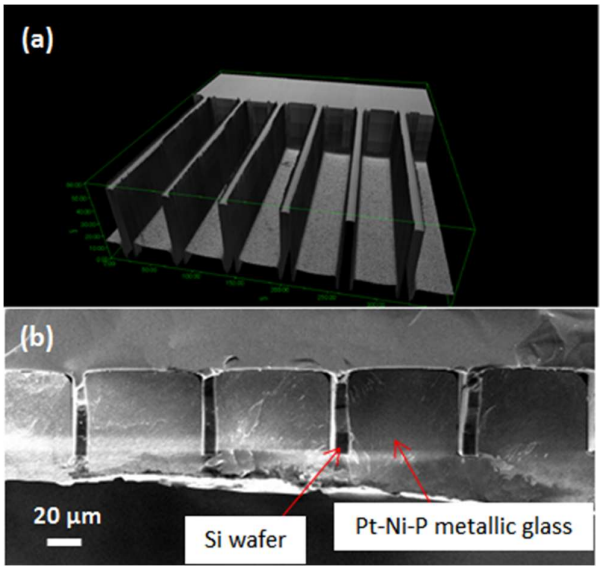

FIG. 4. (a) 3D image of an ICP etched Si mold (close to an edge) obtained by a laser confocal microscope. The pitch of the mask pattern is 72 µm and its depth is 43 µm. (b) SEM image of a CA mask fabricated by imprinting the Pt-metallic glass material into the prepared mold in (a).

Figure 5 shows the illumination curve measured with this setup, which confirms the reasonable performance of this preliminary fabricated mask. Results of the experimental imaging test performed with the imprinted masks are presented in Figure 6. In this figure, the retrieved absorption and differential phase images of four types of rubber cylinders are displayed.

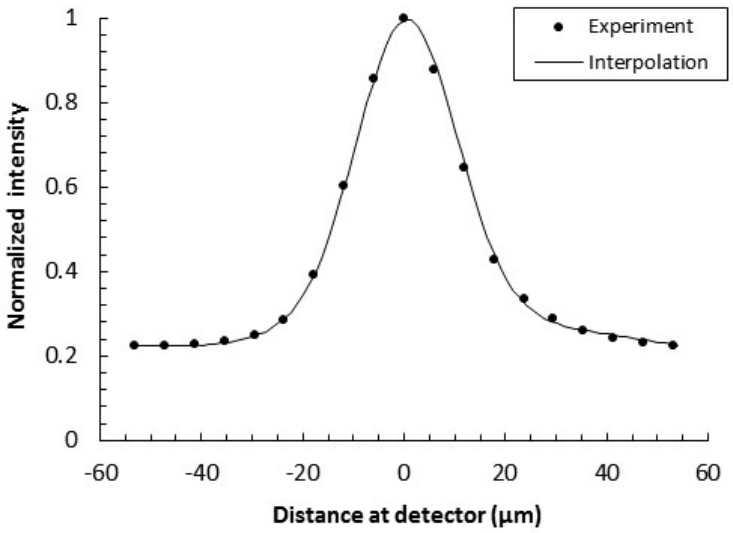

FIG. 5. Measured illumination curve (dots) and interpolated curve to the data points (solid line) for the EI XPCI system

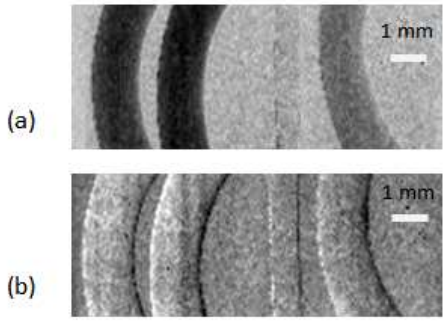

FIG. 6. X-ray absorption (a) and differential phase (b) image of four different rubber cylinders of NBR-70-1, FKM-70, polyurethane, and VMQ-70, respectively from left to right, which were acquired with an EI XPCI system based on the new fabricated metallic glass masks.

In some cases, there may be a few microns of the metallic glass layer left on the masks' surface (see Figure 2(e)) which would lead to hardening the X-ray beam, and thus affect the image contrast. These are because of the decrease in the refractive index with x-ray energy as well as of increased offset in the illumination curve. This additional layer can be easily removed by fine polishing the mask surface, which also makes it more uniform and reduces the potential unwanted refraction from irregularities on the mask surface itself. If the metallic glass material has already crystallized, the mask surface can still be treated with an Ar-ion milling machine. Furthermore, by separation of the Si mold from the absorbing septa through

an etching process or thinning the Si mold, as described in previous studies[23,32], it would be possible to eliminate another source of extra absorption.

V. CONCLUSION

In this work, the possibility of using metallic glass masks for EI XPCI was studied. For this purpose, two absorption masks were fabricated from a Pt-based metallic glass material through an imprinting process. Compared to previous metallic glass gratings used in another XPCI method (i.e. X-ray grating interferometry), the alloy takes advantages from Platinum element which leads to higher X-ray attenuation as well as higher glass formability. The latter characteristic facilitates the mask fabrication in lower pressures and temperatures, while practically poses no limits on the pitch, depth, or FOV of such masks. The only parameter that restricts the mask area is the size of the head and plate of the imprinting machine. Since there are already machines with large head sizes, the fabrication of masks for desirable imaging size are technically feasible. Another vantage point of the adopted method is that it can be implemented within a few minutes even on large mask areas with high metallic glass thicknesses. It should also be noted that this method is very cost-effective. This is very important when compared with the fabrication process commonly used to produce micro-structured absorption gratings, e.g. gold electroplating, which is time-consuming, expensive, and less efficient, particularly for large fields of view and high aspect ratios. We performed an imaging experiment with the fabricated masks by including them in an EI XPCI (CA XPCI) system in order to test the performance of the system with those masks. Absorption and differential phase images were successfully retrieved from frames acquired with this setup. The experimental results demonstrated the potential application of this method for fabricating CA masks with the desirable quality in large FOVs at low cost in future.

ACKNOWLEDGEMENT

We would like to highly appreciate Dr. Hidekazu Takano at Tohoku University for his kind helps and useful discussions.

[1] A. Olivo and E. Castelli, " X-ray phase contrast imaging: From synchrotrons to conventional sources," Riv. Nuovo Cim. **37(9)**, 467 (2014).

[2] A. Momose, " Recent Advances in X-ray Phase Imaging," Jpn. J. Appl. Phys. **44(49)**, 6355 (2005).

[3] Y. Takeda, W. Yashiro, T. Hattori, A. Takeuchi, Y. Suzuki, and A. Momose, " Differential phase X-ray imaging microscopy with X-ray Talbot interferometer," Appl. Phys. Express **1(11)**, 117002 (2008).

[4] A. Momose, W. Yashiro, K. Kido, J. Kiyohara, C. Makifuchi, T. Ito, S. Nagatsuka, C. Honda, D. Noda, T. Hattori, T. Endo, M. Nagashima, and J. Tanaka, " X-ray phase imaging: from synchrotron to hospital," Philos. Trans. A. Math. Phys. Eng. Sci. **372**, 20130023 (2014).

[5] A. Snigirev, I. Snigireva, V. Kohn, S. Kuznetsov, and I. Schelokov," On the possibilities of x-ray phase contrast microimaging by coherent high-energy synchrotron radiation," Rev. Sci. Instrum. **66**, (1995).

[6] D. Chapman, W. Thomlinson, R.E. Johnston, D. Washburn, E. Pisano, N. Gmür, Z. Zhong, R. Menk, F. Arfelli, and D. Sayers, " Diffraction enhanced x-ray imaging," Phys. Med. Biol. **42(11)**, 2015 (1997).

[7] A. Momose, " Phase-sensitive imaging and phase tomography using X-ray interferometers," Opt. Express **11(19)**, 2303 (2003).

[8] F. Pfeiffer, M. Bech, O. Bunk, P. Kraft, E.F. Eikenberry, C. Brönnimann, C. Grünzweig, and C. David, "Hard-X-ray dark-field imaging using a grating interferometer, " Nat. Mater. **7**, 134 (2008).

[9] Z.F. Huang, K.J. Kang, L. Zhang, Z.Q. Chen, F. Ding, Z.T. Wang, and Q.G. Fang, " Alternative method for differential phase-contrast imaging with weakly coherent hard x rays," Phys. Rev. A - At. Mol. Opt. Phys. **79**, 1 (2009).

[10] P.C. Diemoz, M. Endrizzi, C.K. Hagen, C. Rau, A. Bravin, R.D. Speller, I.K. Robinson, and A. Olivo, " Edge illumination X-ray phase-contrast imaging: nanoradian sensitivity at synchrotrons and translation to conventional sources," J. Phys. Conf. Ser. **499(1)**, 12006 (2014).

[11] T. Hou, I. Zanette, M.-C.Z. Dora, U. Undström, D.H. Larsson, H.M. Hertz, F. Pfeiffer, and A. Burvall, " Speckle-based x-ray phase-contrast imaging with a laboratory source and the scanning technique," Opt. Lett. **40(12)**, 2822 (2015).

[12] K.J. Harmon, H. Miao, A.A. Gomella, E.E. Bennett, B.A. Foster, P. Bhandarkar, and H. Wen, " Motionless electromagnetic phase stepping versus mechanical phase stepping in x-ray phase-contrast imaging with a compact source," Phys. Med. Biol. **60(8)**, 3031 (2015).

[13] A. Olivo, F. Arfelli, G. Cantatore, R. Longo, R.H. Menk, S. Pani, M. Prest, P. Poropat, L. Rigon, G. Tromba, E. Vallazza, and E. Castelli, " An innovative digital imaging set-up allowing a low-dose approach to phase contrast applications in the medical field," Med Phys **28(8)**, 1610 (2001).

[14] A. Olivo and R. Speller," A coded-aperture technique allowing x-ray phase contrast imaging with conventional sources," Appl. Phys. Lett. **91**, 1 (2007).

[15] P.R. Munro, L. Rigon, K. Ignatyev, F.C. Lopez, D. Dreossi, R.D. Speller, and A. Olivo, " A quantitative, non-interferometric X-ray phase contrast imaging technique," Opt Express **21(1)**, 647 (2013).

[16] A. Olivo and R. Speller," Modelling of a novel x-ray phase contrast imaging technique based on coded apertures," Phys Med Biol **52(22)**, 6555 (2007).

[17] G.K. Kallon, M. Wesolowski, F.A. Vittoria, M. Endrizzi, D. Basta, T.P. Millard, C. Paul, and A. Olivo, "Directional sensitivity A laboratory based edge-illumination x-ray phase-contrast imaging setup with two-directional sensitivity," Appl. Phys. Lett. **107(20)**, 204105 (2015).

[18] M. Endrizzi, A. Astolfo, F.A. Vittoria, T.P. Millard, and A. Olivo, " Asymmetric masks for laboratory-based X-ray phase-contrast imaging with edge illumination," Sci. Rep. **6**, 25466 (2016).

[19] P.R.T. Munro, K. Ignatyev, R.D. Speller, and A. Olivo, " Phase and absorption retrieval using incoherent X-ray sources," Proc. Natl. Acad. Sci. **109(35)**, 13922 (2012).

[20] C. David, J. Bruder, T. Rohbeck, C. Grünzweig, C. Kottler, a. Diaz, O. Bunk, and F. Pfeiffer, "

Fabrication of diffraction gratings for hard X-ray phase contrast imaging," Microelectron. Eng. **84**, 1172 (2007).

[21] D. Noda, M. Tanaka, K. Shimada, and T. Hattori, " Fabrication of Diffraction Grating with High Aspect Ratio Using X-ray Lithography Technique for X-ray Phase Imaging," Jpn. J. Appl. Phys. **46(2)**, 849 (2007).

[22] D. Noda, M. Tanaka, K. Shimada, W. Yashiro, A. Momose, and T. Hattori, " Fabrication of large area diffraction grating using LIGA process," Microsyst. Technol. **14(9-11)**, 1311 (2008).

[23] S. Rutishauser, M. Bednarzik, I. Zanette, T. Weitkamp, M. Börner, J. Mohr, and C. David, " Fabrication of two-dimensional hard X-ray diffraction gratings," Microelectron. Eng. **101**, 12 (2013).

[24] F. Koch, T. Schröter, D. Kunka, P. Meyer, J. Meiser, M.I. Khalil, L. Birnbacher, M. Viermetz, M. Walter, J. Schulz, F. Pfeiffer, and J. Mohr, " Gratings on low absorption substrates for X-ray Phase Contrast Imaging," Rev. Sci. Instrum. **86(12)**, 38 (2015).

[25] J. Kenntner, T. Grund, B. Matthis, M. Boerner, J. Mohr, T. Scherer, M. Walter, M. Willner, A. Tapfer, M. Bech, F. Pfeiffer, I. Zanette, and T. Weitkamp, " Front- and backside structuring of gratings for phase contrast imaging with x-ray tubes," Proc. SPIE **7804**, 780408 (2010).

[26] J. Mohr, T. Grund, D. Kunka, J. Kenntner, J. Leuthold, J. Meiser, J. Schulz, and M. Walter, " High aspect ratio gratings for X-ray phase contrast imaging," AIP Conf. Proc. **1466**, 41 (2012).

[27] J. Baborowski, V. Revol, C. Kottler, R. Kaufmann, P. Niedermann, F. Cardot, A. Dommann, A. Neels, and M. Despont, " High aspect ratio, Large area silicon-based gratings for X-ray phase contrast imaging," 2014 IEEE 27th Int. Conf. Micro Electro Mech. Syst. 490 (2014).

[28] J. Meiser, M. Amberger, M. Willner, D. Kunka, P. Meyer, F. Koch, a. Hipp, M. Walter, F. Pfeiffer, and J. Mohr, " Increasing the field of view of x-ray phase contrast imaging using stitched gratings on low absorbent carriers," SPIE Med. Imaging **1**, 903355 (2014).

[29] T.J. Schröter, F. Koch, P. Meyer, M. Baumann, D. Münch, D. Kunka, S. Engelhardt, M. Zuber, T. Baumbach, and J. Mohr, " Large area gratings by x-ray LIGA dynamic exposure for x-ray phase-contrast imaging," J. Micro/Nanolithography, MEMS, MOEMS **16(1)**, 13501 (2017).

[30] K. Wan, Y. Takeda, W. Yashiro, and A. Momose, " Fabrication of multiple slit using stacked-sliced method for hard X-ray Talbot–Lau interferometer," Jpn. J. Appl. Phys. **47(9R)**, 7412 (2008).

[31] S.K. Lynch, C. Liu, N.Y. Morgan, X. Xiao, A.A. Gomella, D. Mazilu, E.E. Bennett, L. Assoufid, F. de Carlo, and H. Wen, " Fabrication of 200 nm period centimeter area hard x-ray absorption gratings by multilayer deposition," J. Micromechanics Microengineering **22(10)**, 105007 (2012).

[32] W. Yashiro, D. Noda, T. Hattori, K. Hayashi, A. Momose, and H. Kato, " A metallic glass grating for X-ray grating interferometers fabricated by imprinting," Appl. Phys. Express **7(3)**, 032501 (2014).

[33] W. Yashiro, K. Kato, M. Sadeghilaridjani, A. Momose, T. Shinohara, and H. Kato, " X-ray phase imaging using a Gd-based absorption grating fabricated by imprinting technique," Jpn. J. Appl. Phys. **55(4)**, 048003 (2016).

[34] Y. Lei, Y. Du, J. Li, Z. Zhao, X. Liu, J. Guo, and H. Niu, " Fabrication of x-ray absorption gratings via micro-casting for grating-based phase contrast imaging," J. Micromechanics Microengineering **24(1)**, 15007 (2014).

[35] Y. Lei, X. Liu, J. Li, J. Guo, and H. Niu, " Improvement of filling bismuth for x-ray absorption gratings through the enhancement of wettability," J. Micromechanics Microengineering **26(6)**, 65011 (2016).

[36] Y.C. Weng, Y.J. Weng, H.S. Fang, and S.Y. Yang, " Electromagnetic imprint technique combined with

electrophoretic deposition technique in forming microelectrode structures," Jpn. J. Appl. Phys. **50(4R)**, 46502 (2011).

[37] Y. Fukuda, Y. Saotome, N. Nishiyama, K. Takenaka, N. Saidoh, E. Makabe, and A. Inoue, " Fabrication of nanodot array mold with 2 Tdot/in.2 for nanoimprint using metallic glass," J. Vac. Sci. Technol. BNanotechnology Microelectron. **30(6)**, (2012).

[38] Y. Saotome, S. Miwa, T. Zhang, and A. Inoue, " The micro-formability of Zr-based amorphous alloys in the supercooled liquid state and their application to micro-dies," J. Mater. Process. Technol. **113(1-3)**, 64 (2001).

[39] P.C. Diemoz, C.K. Hagen, M. Endrizzi, and A. Olivo," Sensitivity of laboratory based implementations of edge illumination X-ray phase-contrast imaging," Appl. Phys. Lett. **103**, 244104 (2013).